

Self-Supervised Modality-Aware Multiple Granularity Pre-Training for RGB-Infrared Person Re-Identification

Lin Wan¹, Qianyan Jing¹, Zongyuan Sun¹, Chuang Zhang², Zhihang Li^{3,*}, Yehansen Chen^{1,*}

¹School of Geography and Information Engineering, China University of Geosciences (Wuhan)

²School of Computer Science and Engineering, Nanjing University of Science and Technology

³School of Artificial Intelligence, University of Chinese Academy of Sciences

Abstract

While RGB-Infrared cross-modality person re-identification (RGB-IR ReID) has enabled great progress in 24-hour intelligent surveillance, state-of-the-arts still heavily rely on fine-tuning ImageNet pre-trained networks. Due to the single-modality nature, such large-scale pre-training may yield RGB-biased representations that hinder the performance of cross-modality image retrieval. This paper presents a self-supervised pre-training alternative, named Modality-Aware Multiple Granularity Learning (MMGL), which directly trains models from scratch on multi-modality ReID datasets, but achieving competitive results without external data and sophisticated tuning tricks. Specifically, MMGL globally maps shuffled RGB-IR images into a shared latent permutation space and further improves local discriminability by maximizing agreement between cycle-consistent RGB-IR image patches. Experiments demonstrate that MMGL learns better representations (+6.47% Rank-1) with faster training speed (converge in few hours) and solidier data efficiency (<5% data size) than ImageNet pre-training. The results also suggest it generalizes well to various existing models, losses and has promising transferability across datasets. The code will be released.

1 Introduction

It is not a secret that today's success of person re-identification (ReID) is mainly owed to the accumulation of visible images. Deep models trained with RGB data have spawned beyond-human performance over various benchmarks [Zheng *et al.*, 2015]. Despite of these advances, it is worth noting that visible cameras are sensitive to illumination variations, often failing to capture valid visual information in low lighting conditions (*e.g.*, at night). Fortunately, owing to the inherent illumination robustness, infrared (IR) images provide effective complement for building a 24-hour ReID system. This has attracted considerable attention to pedestrian retrieval across RGB and IR sensing modalities, *i.e.*, RGB-IR ReID [Wu *et al.*, 2017].

*Equally-contributed corresponding authors

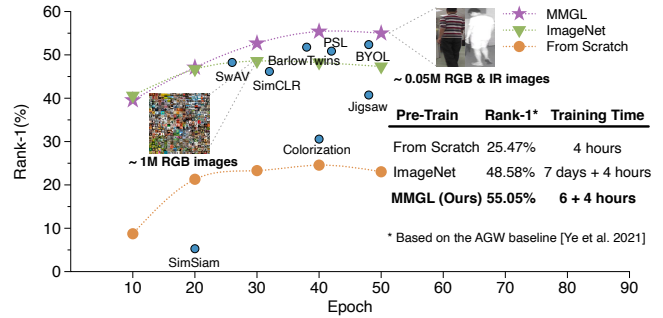


Figure 1: Comparison of Modality-Aware Multiple Granularity (MMGL) and ImageNet pre-training. MMGL boosts performance with solid data efficiency and also outperforms other self-supervised methods. Times are measured on an Nvidia 2080Ti GPU.

Facing the lack of large-scale public datasets, pre-training backbones on ImageNet [Deng *et al.*, 2009], and then fine-tuning on target datasets has become a de-facto paradigm for ReID tasks [Ye *et al.*, 2021b]. However, in RGB-IR ReID, the domain shift between ImageNet and target multi-modality datasets is so large that the marginal benefit from large-scale data [He *et al.*, 2019] is partly counteracted by the *modality bias training* issue [Huang *et al.*, 2021]. Huge amounts of pre-learned RGB information could overwhelm the ‘scarce’ IR spectrum during fine-tuning, leading to biased representations. Recently, starting from ImageNet pre-trained checkpoints, [Ye *et al.*, 2021b] present state-of-the-art results for different ReID tasks. It achieves 95% Rank-1 accuracy for single-modality ReID, but small performance gains on RGB-IR datasets (see Fig. 1, Rank-1 increases only from 25% to 48%). This motivates us to think — *Is ImageNet pre-training the only starting point for cross-modality image retrieval?*

One intuitive alternative might be ‘without pre-training’, but ‘training from scratch’ is almost impossible owing to the notorious *over-fitting* problem. As shown by the brown line in Fig. 1, directly training on RGB-IR ReID datasets from random initialization has not achieved competitive results as [He *et al.*, 2019]. To mitigate over-fitting, [Fu *et al.*, 2021] perform unsupervised pre-training on a huge LUPerson dataset, gaining significant performance boost on mainstream ReID tasks. However, such improvement still heavily relies on *expensive* human-collected data. Besides, this dataset also only

contains RGB data, which is unable to alleviate the above-mentioned *modality bias training* issue.

This paper questions *modality bias training* and *expensive pre-training* by exploring a novel regime: we report that competitive cross-modality ReID accuracy is achievable when directly pre-training on *target RGB-IR datasets, without additional data and manual labels*. More interestingly, we even *surpass* ImageNet supervised pre-training by a large margin with $<5\%$ data size ($0.05M$ vs. $1M$) and no sophisticated tuning tricks. The secret to our success lies in two novel designs. **First**, we develop a *permutation recovery* pretext task, training an encoder end-to-end to recover the original order of randomly shuffled person images. By globally mapping RGB-IR image pairs into the same permutations, a shared permutation latent space will be learned to narrow the distribution gap between RGB and IR pixels, yielding modality-invariant representations. **Second**, based on the shuffled image patches, we further advance a part-aware cycle-contrastive learning strategy to capture fine-grained visual cues at the local granularity. Given a specific patch, we treat it as a query to derive two attentive representations within/across modality using soft nearest neighbor retrieval. The retrieved patches form a cycle between modalities, acting as a positive pair for contrastive learning [Hjelm *et al.*, 2018]. Employing such cross-modality cycle-consistency enables contrastive learning for unpaired multi-modal images, effectively improving the local discriminability of learned representations. Compared to prior work [Fu *et al.*, 2021], our formulation uses natural cross-modality correlations to avoid laborious data collection and augmentation, allowing efficient RGB-IR ReID.

When directly pre-training a simple baseline from scratch [Ye *et al.*, 2021b], our MMGL paradigm achieves **6.47% absolute improvement** over its ImageNet counterpart (Fig. 1, Purple Line). Extensive experiments demonstrate that this comparability is retained when applying MMGL to various state-of-the-arts. Furthermore, the pre-trained models also show better generalization capability in cross-dataset settings. Our contributions are three-fold: (1) We are the first to explore pre-training solutions for RGB-IR ReID and pioneer a non-ImageNet-powered paradigm MMGL to enable self-supervised pre-training directly on target datasets, effectively solving the *modality bias training* issue with promising data efficiency. (2) We propose a part-aware cycle-contrastive learning strategy to increase the discriminability of cycle-consistent RGB-IR patches, significantly improving performance of RGB-IR ReID. (3) We conduct extensive experiments to show the good generalization ability of MMGL over various state-of-the-art models, losses, and datasets.

2 Related Work

RGB-IR Person ReID focuses efforts in tackling pixel and feature misalignment issues between modalities. Currently, there are mainly two lines of literature: image synthesis and shared feature learning. Image synthesis methods usually adopt generative adversarial networks (GAN) [Goodfellow *et al.*, 2014] to minimize pixel-level difference across modality by synthesizing IR/RGB counterparts for RGB/IR images. Following this vein, [Wang *et al.*, 2019] firstly propose

to combine pixel and feature alignment to learn modality-invariant and discriminative representations. Several studies also apply cross-modality paired image synthesis [Wang *et al.*, 2020], feature disentanglement [Choi *et al.*, 2020], and intermediate modality generation [Li *et al.*, 2020] to enhance the quality of generated images. However, it is ill-posed for GAN-based methods to recover color appearances for IR images, resulting in the deficiency of identity information in fake RGB images [Ye *et al.*, 2019]. Shared feature learning attempts to discover a common feature subspace to align modality distributions. [Wu *et al.*, 2017] first release a multi-modal ReID dataset (SYSU-MM01) and present a deep zero-padding network for RGB-IR ReID. [Ye *et al.*, 2021a] propose a two-stream network to extract shared features. Recently, various feature selection approaches are designed to enhance representation discriminability, including graph neural networks [Ye *et al.*, 2020] and automated feature search [Chen *et al.*, 2021b]. However, they all adopt ImageNet pre-training as an outset, suffering from modality bias brought by cross-modality ReID.

Self-Supervised Learning (SSL) is currently the fastest-growing branch of unsupervised learning, which is mainly exploited to pre-train network to solve a pre-designed *pretext* task, aiming to learn ‘universal’ representations for downstream task from unlabeled raw data using data itself as supervisory signals [Jing and Tian, 2020]. Over the last decade, self-supervised pre-training has witnessed a wide range of pretext task designs based on data generation [Zhang *et al.*, 2016], spatial or temporal contexts [Noroozi and Favaro, 2016], and multi-modal correspondence [Zou *et al.*, 2018]. For various types of self-supervised pretext tasks, contrastive supervision aims to maximize agreement between different data views to forge a discriminative feature subspace [Caron *et al.*, 2020; Grill *et al.*, 2020; Zbontar *et al.*, 2021; Chen *et al.*, 2021a; Chen and He, 2021], which is proved effective in learning high quality representations for downstream tasks [Chen *et al.*, 2020; He *et al.*, 2020]. Nevertheless, contrastive correspondence is hard to be mined in multi-modal ReID scenarios due to the unpaired nature of heterogeneous images. In this paper, we leverage cycle-consistency [Zhu *et al.*, 2017] between human body parts to enable contrastive learning for RGB-IR ReID.

3 Methodology

Prior work [Ye *et al.*, 2020] suggests that ‘universe’ RGB-IR ReID representations should be both modality-invariant and discriminative. This motivates two novel designs of our MMGL pre-training paradigm: (a) *Permutation Recovery* pretext task that maps randomly shuffled RGB-IR image pairs into a shared permutation latent space for global invariant learning. (b) *Part-aware Cycle-Contrastive Learning* strategy that maximizes agreement between cycle-consistent RGB-IR image patches to improve local discriminability. Fig. 2 illustrates the idea, introduced next.

3.1 Cross-Modality Permutation Recovery

As shown in Fig. 2, given a ranking vector \hat{O} that represents a randomly shuffled image patch sequence, the permutation

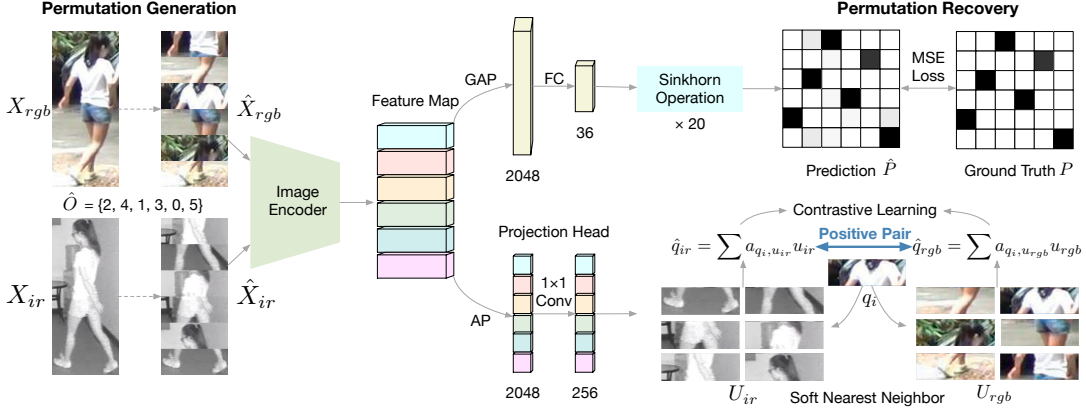


Figure 2: An overview of the proposed Modality-Aware Multiple Granularity Learning (MMGL) pipeline. Generally, MMGL consists of a permutation recovery branch and a cycle-contrast branch at global and local granularities respectively. The former aims to learn a shared permutation latent space by recovering the original order of each cross-modality shuffled image pair. The latter seeks to enhance patch discriminative power by maxing the agreement between patch representations derived with cross-modality cycle-consistency.

recovery task aims to learn to reconstruct its original counterpart O with a *permutation matrix* P [Mena *et al.*, 2018]. Mathematically, P belongs to the set of 0-1 doubly stochastic matrices, where each non-zero element in the i -th row and j -th column suggests that the current i -th patch should be assigned to the j -th place of the sequence. This leads to a regression problem $O = P_{\Theta, \hat{O}}^{-1} \hat{O}$, where we seek to derive P with network parameters Θ . However, the discrete nature of this problem may pose great challenges to the model optimization. Here, we present how to approximate this task solving process in the context of backpropagation.

Permutation Generation. We introduce a modality-shared shuffling operator $G(X_{rgb}, X_{ir}, \hat{O})$ that transforms randomly composed cross-modality image pairs $\{X_{rgb}, X_{ir}\}$ to their shuffled counterparts $\{\hat{X}_{rgb}, \hat{X}_{ir}\}$ (see Fig. 2, left). Suppose the shuffled image contains N patches, \hat{O} is then a random permutation of an array $[1, \dots, N]$ sampled from the uniform distribution, which denotes the mapping from original image patches to their randomly shuffled patches. For each image with H height and W width, the shuffling generates a rearranged sequence of image patches (with size of $H/N \times W$) by choosing the i -th patch from \hat{O}_i position of the original sequence. Note that \hat{O} is shared within each cross-modality image pair, which maps both modality images into a common permutation subspace. This is beneficial to learn invariant features for global modality alignment.

Permutation Recovery. We map shuffled images to corresponding affinity matrices $\hat{P} \in \mathbb{R}^{N \times N}$ to recover their original orders. Such mappings can be fitted by an encoder $\mathcal{F}(\hat{X}_{rgb}, \hat{X}_{ir}, \Theta)$ with parameters Θ that transforms each image into a N^2 -dim feature representation. Specifically, for each $\{\hat{X}_{rgb}, \hat{X}_{ir}\}$, \mathcal{F} learns two global representations f_{rgb} and f_{ir} . We then reduce their dimensions to N^2 using a shared fully-connected layer \mathcal{G} , i.e., $\hat{f}_{rgb}, \hat{f}_{ir} = \mathcal{G}(f_{rgb}, f_{ir})$. It is worth noting that the selection of \mathcal{F} should be consonant

with downstream supervised models. We transform \hat{f} into a $N \times N$ matrix \hat{P} , in which each row and column can be regarded as a logit vector that denotes the possibility of a patch belonging to a serial position (i.e., a category).

Nevertheless, it is tough to directly fit permutation matrix P with the learned \hat{P} , because each patch is discrete, making the approximation process non-differentiable. To this end, we introduce the Gumbel-Sinkhorn operator [Mena *et al.*, 2018] to relax \hat{f} to the continuous domain so as to fit a categorical distribution. The Sinkhorn operator is defined as:

$$\begin{aligned} \text{Sinkhorn}^0(\hat{P}) &= \exp(\hat{P}), \\ \text{Sinkhorn}^l(\hat{P}) &= \mathcal{T}_c \left(\mathcal{T}_r \left(\text{Sinkhorn}^{l-1}(\hat{P}) \right) \right), \\ \text{Sinkhorn}(\hat{P}) &= \lim_{l \rightarrow \infty} \text{Sinkhorn}^l(\hat{P}), \end{aligned} \quad (1)$$

where $\mathcal{T}_r(\hat{P}) = \hat{P} \oslash (\hat{P} \mathbf{1}_N \mathbf{1}_N^\top)$, $\mathcal{T}_c(\hat{P}) = \hat{P} \oslash (\mathbf{1}_N \mathbf{1}_N^\top \hat{P})$ indicates the row and column-wise normalization of a matrix respectively, \oslash means element-wise division, $\mathbf{1}_N$ is a column vector of ones, l is the number of iterations.

Based on the Sinkhorn operator, we can reparameterize the hard choice of the permutation matrix with Gumbel-Softmax distribution [Jang *et al.*, 2016]:

$$\text{G-Sinkhorn}(\hat{P}/\tau) = \text{softmax}((\text{trace}(\hat{P}^\top \hat{P}) + \gamma)/\tau), \quad (2)$$

where γ denotes random noises sampled from a Gumbel distribution, τ is the temperature hyperparameter.

After relaxing the learned affinity matrix \hat{P} , we could gradually approach the ground truth P via backpropagation, leading to the following permutation reconstruction error:

$$\mathcal{L}_p = \sum_{i=1}^M \left\| O_i - \hat{P}^{-1} \hat{O}_i \right\|^2, \quad (3)$$

where M is the size of a mini-batch, O and \hat{O} is the original/shuffled ranking vector, respectively.

3.2 Part-Aware Cycle-Contrastive Learning

With cross-modality permutation recovery, the pre-trained model is able to learn modality-invariant biometrics (e.g., shape and texture) in favour of modality alignment. However, it may collapse to *low-loss* solutions that hinder it learning desired representations, e.g., directly utilizing boundary patterns and textures continuing across patches to solve the task. Such ‘shortcuts’ will suppress the intra-class compactness, leading to fuzzy decision boundaries for identity recognition.

Recent advances on contrastive learning show its promising capability in learning discriminative representations [Chen *et al.*, 2020; He *et al.*, 2020]. With delicately designed data augmentation strategies, it maximizes the agreement between different views of the same image to achieve better intra-class compactness and inter-class discriminability. Nonetheless, due to the unpaired nature of heterogeneous images in our task, it is infeasible to directly apply off-the-shelf contrastive learning pipelines to multi-modal scenarios. As most augmentations are intra-modality, they also can not reflect cross-modality correlations of identity semantics.

Here, we propose a part-aware cycle-contrastive (PCC) constraint that uses cross-modality cycle consistency to enable contrastive learning at the local granularity. For each image patch, we utilize a *PCB-style* projection head [Sun *et al.*, 2019] to map it into a normalized 256-dim representation (see Fig. 2, lower branch). After projection, we introduce a forward-backward nearest neighbor process to capture cross-modality cycle-consistency. Given a query representation q_i , we first derive its soft nearest neighbor \hat{q} from the universal representation set U of counterpart modality. Then, we compute the soft nearest neighbor of \hat{q} backwards within the patch set of the same image. The cycle-consistency is satisfied when the two retrieved soft nearest neighbors are similar. The retrieval process is defined as:

$$\hat{q}_i = \sum_{u \in U} \alpha_{q_i, u} u, \quad \alpha_{q_i, u} = \frac{\exp(\text{sim}(q_i, u) / \tau)}{\sum_{u' \in U} \exp(\text{sim}(q_i, u') / \tau)}, \quad (4)$$

where τ is the temperature and sim is the cosine similarity.

After the similarity-based forward-backward retrieval, we would obtain a cross-modality patch pair $\{\hat{q}_{ir}, \hat{q}_{rgb}\}$ with similar semantics and two sets of retrieved representations $\{V_{ir}, V_{rgb}\}$. We regard $\{\hat{q}_{ir}, \hat{q}_{rgb}\}$ as a positive pair while $\{V_{ir}, V_{rgb}\}$ as negative sets for contrastive learning:

$$\mathcal{L}_{\text{PCC}} = -\log \frac{\exp(\text{sim}(\hat{q}_{ir}, \hat{q}_{rgb}) / \tau)}{\sum_{u \in \{V_{ir}, V_{rgb}\}} \exp(\text{sim}(\hat{q}_i, u) / \tau)}. \quad (5)$$

By pulling together $\{\hat{q}_{ir}, \hat{q}_{rgb}\}$ whilst pushing away all negative pairs, the deep network will learn to discover modality correspondence across semantic-similar body partitions. This explicit supervision facilitates the fine-grained alignment of heterogeneous images, helping to transfer better modality invariance and discriminative power to downstream cross-modality ReID models.

The overall learning objective of MMGL is formulated as:

$$\mathcal{L}_{\text{MMGL}} = \mathcal{L}_p + \lambda \mathcal{L}_{\text{PCC}}, \quad (6)$$

where λ is a trade-off factor to balance each objective.

3.3 Supervised Fine-Tuning for RGB-IR ReID

In the fine-tuning stage, we transfer the MMGL pretrained backbone to downstream models and perform supervised learning for cross-modality image retrieval. Following existing RGB-IR ReID studies [Ye *et al.*, 2020], we optimize the identity cross-entropy loss \mathcal{L}_{id} and triplet loss $\mathcal{L}_{\text{triplet}}$ [Hermans *et al.*, 2017] as follow:

$$\mathcal{L}_{\text{ReID}} = \mathcal{L}_{\text{id}} + \mathcal{L}_{\text{triplet}}. \quad (7)$$

4 Experiments

We evaluate MMGL on standard RGB-IR ReID benchmarks. Please refer to the **Appendix** for more experimental results.

4.1 Datasets and Evaluation Protocols

Datasets. Our experiments are based on SYSU-MM01 [Wu *et al.*, 2017] and RegDB [Nguyen *et al.*, 2017] benchmarks.

SYSU-MM01 is the current largest RGB-IR ReID dataset collected by 4 RGB and 2 IR cameras. Statistically, the training set contains 22,258 RGB and 11,909 IR images of 395 persons, while the testing set is divided into a query set including 3,803 IR images and a RGB gallery set (96 identities both). The gallery set has two versions according to evaluation modes. In the *indoor search* mode, only images captured by two indoor cameras are involved. For the *all search* mode, all images obtained by four RGB cameras are used.

RegDB is a relatively tiny dataset acquired by a dual-camera system (i.e., paired RGB and thermal cameras). It includes 412 persons, where each person has 10 visible and 10 thermal images, respectively. Randomly sampled 206 persons’ images are used for training while the others are employed for testing. There are also two evaluation modes, i.e., *visible-thermal* and *thermal-visible*, by alternatively using all visible/thermal images as the query set.

Evaluation Protocols. We adopt the standard RGB-IR ReID evaluation protocols [Ye *et al.*, 2020] and use the Cumulative Matching Characteristic (CMC) and mean Average Precision (mAP) as evaluation metrics. Following [Wu *et al.*, 2017], experimental results on SYSU-MM01 are based on the average of ten random splits of the gallery and query set. Following [Ye *et al.*, 2020], we conduct a 10-fold cross validation on RegDB and report the average performance.

4.2 Implementation Details

We implement MMGL with PyTorch on an Nvidia 2080Ti GPU. All images are resized to 288×144 . An SGD optimizer with 0.9 momentum and 0.0005 weight decay is used for optimization. We set initial learning rate to 0.1 with linear warm-up [Ye *et al.*, 2020] and decay it with the cosine decay schedule without restarts, with a total of 100 epochs.

Pre-Training Stage. For pre-training, we randomly sample 56 RGB and 56 IR images without labels for each training batch. Each image is horizontally split into 6 stripes equally. Conventional random cropping with zero-padding, horizontal flipping, AugMix [Hendrycks *et al.*, 2019] and random erasing [Zhong *et al.*, 2020] are chosen for data augmentation. Following [Mena *et al.*, 2018], we use $l = 20$ for Sinkhorn

Table 1: MMGL with common baselines on SYSU-MM01 with Rank-1, 10, 20 (%) and mAP (%) evaluation metrics.

Method	Venue	Pre-Train	All-Search								Indoor-Search							
			Single-Shot				Multi-Shot				Single-Shot				Multi-Shot			
			r1	r10	r20	mAP	r1	r10	r20	mAP	r1	r10	r20	mAP	r1	r10	r20	mAP
One-Stream	TPAMI 2021	Random Init.	26.29	67.86	81.26	27.28	30.83	73.07	85.53	20.81	26.05	72.15	87.99	36.24	31.39	78.86	91.82	25.96
		ImageNet-1k	43.66	83.92	92.23	43.70	50.16	87.10	94.50	37.20	48.93	89.28	96.40	57.86	56.80	92.47	97.11	49.11
		MMGL (Ours)	50.77	88.01	94.08	49.61	58.77	91.66	96.39	43.13	54.00	91.73	96.77	62.57	62.91	94.01	97.58	53.48
AGW	TPAMI 2021	Random Init.	25.47	66.06	80.11	26.07	32.67	75.81	87.13	22.98	26.38	70.61	86.08	35.95	33.37	80.01	92.15	27.83
		ImageNet-1k	48.58	87.58	94.83	49.37	54.73	92.46	96.72	42.90	54.67	89.56	95.91	42.90	62.13	93.42	97.06	54.56
		MMGL (Ours)	55.05	89.61	95.06	53.05	61.64	93.14	97.33	46.09	58.93	93.23	97.51	66.34	65.35	95.11	97.90	57.04
DDAG	ECCV 2020	Random Init.	fail	fail	fail	fail	fail	fail	fail	fail	fail	fail	fail	fail	fail	fail	fail	fail
		ImageNet-1k	54.75	90.39	95.81	53.02	61.83	92.68	97.49	47.06	61.02	94.06	98.41	67.98	69.23	95.13	98.31	59.42
		MMGL (Ours)	55.65	91.10	96.06	53.51	60.97	92.88	97.53	46.85	59.39	94.32	97.93	66.96	69.20	95.35	98.02	58.89
NFS	CVPR 2021	Random Init.	30.45	71.83	82.97	31.43	34.18	76.63	87.34	25.01	30.03	75.59	89.57	40.38	34.70	82.66	93.16	30.09
		ImageNet-1k	56.91	91.34	96.52	55.45	63.51	94.42	97.81	48.56	62.79	96.53	99.07	69.79	70.03	97.70	99.51	61.45
		MMGL (Ours)	60.83	92.20	97.51	58.36	66.37	96.97	98.58	51.79	66.71	97.83	99.28	71.32	74.57	98.42	99.62	64.31
CAJ	ICCV 2021	Random Init.	fail	fail	fail	fail	fail	fail	fail	fail	fail	fail	fail	fail	fail	fail	fail	fail
		ImageNet-1k	66.62	95.44	98.56	64.04	74.07	96.88	98.93	56.75	71.39	96.81	99.31	76.47	82.11	97.95	99.03	70.22
		MMGL (Ours)	67.82	96.02	98.88	65.25	76.23	97.66	99.29	58.36	74.55	97.88	99.52	78.75	84.32	99.13	99.85	72.42

Table 2: Cross-dataset performance evaluation on RegDB with Rank-1, 10, 20 (%) and mAP (%) metrics.

Method	Venue	Pre-Train	Source	Visible-Thermal				Thermal-Visible			
				r1	r10	r20	mAP	r1	r10	r20	mAP
One-Stream	TPAMI 2021	Random Init.	RegDB	17.04	33.74	44.76	19.81	16.70	33.20	44.37	19.79
		ImageNet	ImageNet-1k	63.17	84.02	91.89	61.32	61.39	83.27	90.99	60.12
		MMGL (Ours)	SYSU-MM01	65.72	85.31	92.25	63.23	64.71	85.28	92.73	63.85
AGW	TPAMI 2021	Random Init.	RegDB	fail	fail	fail	fail	fail	fail	fail	fail
		ImageNet	ImageNet-1k	70.73	86.46	91.41	65.04	69.85	86.31	89.62	63.66
		MMGL (Ours)	SYSU-MM01	73.56	88.01	92.87	68.28	72.75	87.03	90.25	68.03
DDAG	ECCV 2020	Random Init.	RegDB	fail	fail	fail	fail	fail	fail	fail	fail
		ImageNet	ImageNet-1k	69.34	86.19	91.49	63.46	68.06	85.15	90.31	61.80
		MMGL (Ours)	SYSU-MM01	68.51	85.88	90.45	62.73	67.89	85.00	89.64	60.27
NFS	CVPR 2021	Random Init.	RegDB	37.92	63.57	72.83	38.05	37.35	62.81	71.33	37.69
		ImageNet	ImageNet-1k	80.54	91.96	95.07	72.10	77.95	90.45	93.62	69.79
		MMGL (Ours)	SYSU-MM01	82.24	92.38	96.16	74.98	80.32	92.08	94.76	73.91
CAJ	ICCV 2021	Random Init.	RegDB	fail	fail	fail	fail	fail	fail	fail	fail
		ImageNet	ImageNet-1k	83.25	94.29	97.04	77.31	82.63	94.58	97.11	75.96
		MMGL (Ours)	SYSU-MM01	85.51	95.77	98.02	79.03	84.04	95.93	97.38	77.59

operator iterations. For each sample, we generate 10 reconstructions using Gumbel perturbations. Following [He *et al.*, 2020], we set τ to 0.07. And λ is empirically set to 0.2.

Fine-Tuning Stage. For fine-tuning, we drop the *PCB-style* projection head and initialize the model with MMGL checkpoints, while leaving other default settings (e.g., hyperparameters and data augmentation strategies) unchanged. Note that these settings are not customized for MMGL, tuning them likely leads to better results. We leave it to future work.

4.3 RGB-IR ReID with MMGL

We first evaluate the proposed method with five state-of-the-art models, including One-stream and AGW [Ye *et al.*, 2021b], DDAG [Ye *et al.*, 2020], NFS [Chen *et al.*, 2021b], and CAJ [Ye *et al.*, 2021a]. On SYSU-MM01, a random initialized backbone is firstly pre-trained with MMGL. Then we fine-tune the pre-trained checkpoint with default settings to perform supervised RGB-IR ReID. More experiments on other RGB-IR ReID models are provided in the **Appendix**.

As shown in Table 1, when straightforwardly performing supervised training on SYSU-MM01 from random initialization, much inferior accuracy is observed for all methods. DDAG and CAJ even encounter gradient explosion and fail to converge. This suggests serious over-fitting has happened due to insufficient RGB-IR training samples.

Our proposed MMGL pre-training strategy achieves consistent and significant improvement (more than **25%** Rank-

1 and mAP boost in average) over baselines without pre-training. Such performance gains are obtained neither using additional training data nor supervised pre-training. This manifests that the proposed self-learning technique and part-aware cycle-contrastive constraint provide data-efficient and powerful regularization to prevent over-fitting.

More strikingly, MMGL pre-trained model even outperforms its ImageNet-supervised counterpart on most state-of-the-arts. This indicates that elimination of modality bias has huge positive effects on cross-modality ReID. Furthermore, the promising results on AGW and NFS demonstrate that MMGL is robust to different backbones and loss functions.

Another noteworthy feature of our approach is its fast convergence speed. As shown in Fig. 1, when pre-training on SYSU-MM01 with AGW baseline, MMGL has greatly reduced the amount of training time ImageNet model takes from seven days to four hours, while without any increase in fine-tuning. This results in more efficient RGB-IR ReID.

4.4 Generalization Ability across Datasets

We further evaluate the cross-dataset generalization capability of MMGL features. Specifically, we pre-train the aforementioned five models with MMGL on SYSU-MM01, and then transfer the learned features to solve RGB-IR ReID on RegDB. We use the same fine-tuning hyperparameters ImageNet-supervised model has, and provide random initialization results as references. More transfer learning results

are included in the **Appendix**.

Table 2 shows the fine-tuning results on RegDB. The performance gap between no pre-training and ImageNet pre-training widens more than that on SYSU-MM01, possibly owing to the even smaller size of RegDB. Severe over-fitting also makes it hard to train models from scratch — AGW, DDAG, and CAJ even meet gradient explosion on RegDB.

Surprisingly, MMGL pre-training demonstrates consistent performance and good transferability across datasets, and even surpasses its ImageNet-supervised counterpart when outfitted on various off-the-shelf models. Note that such improvement is achieved under large domain shift, as SYSU-MM01 is captured by near-infrared cameras while RegDB is collected by far-infrared sensors. All of the above results suggest that MMGL features are robust and generalizable.

4.5 Ablation Studies

We evaluate the effectiveness of each MMGL component on the SYSU-MM01 dataset in both *all search* and *indoor search* modes. For fair comparison, all ablations are conducted on AGW baseline [Ye *et al.*, 2021b] with fixed default hyperparameters. Specifically, \mathcal{P} denotes the permutation recovery, and \mathcal{C} represents the PCC constraint (Eq. 5).

Table 3: Ablation Studies on SYSU-MM01.

Pre-Train	All-Search			Indoor-Search		
	r1	r10	mAP	r1	r10	mAP
Rand Init	25.47	66.06	26.07	26.38	70.61	35.95
ImageNet-1k	48.58	87.58	49.37	54.73	92.46	63.72
\mathcal{P}	50.99	88.25	49.77	55.53	91.29	63.33
$\mathcal{P} + \mathcal{C}$	55.05	89.61	53.05	58.93	93.23	66.34

As shown in Table 3, when only pre-training with the \mathcal{P} task, AGW presents encouraging performance even better than ImageNet pre-training. One possible explanation is that permutation recovery task explicitly exploits body typology, a natural supervision being invariant to both modalities for pre-training. Each cross-modality image pair is mapped into a shared permutation latent space where modality distributions can be better-aligned. It is noteworthy that this result is achieved without extra data and labels, suggesting that supervised pre-training on large RGB image sets does not bring much improvement to downstream cross-modality tasks.

Note that performance boost by sole permutation recovery is modest, as the model may easily find undesired trivial solutions, *e.g.*, by directly exploiting boundary patterns of patches to solve the task. Surprisingly, when imposing the proposed PCC constraint on patch embeddings ($\mathcal{P} + \mathcal{C}$), significant improvement can be observed (**+3.70%** Rank-1, **+3.21%** mAP). On the one hand, it offers discriminative features via patch discrimination. On the other hand, it ensures invariance by attracting cycle-retrieved RGB-IR pairs.

4.6 Comparison with Other SSL Methods

We compare MMGL with eight self-supervised learning methods on the SYSU-MM01 dataset. The involved methods can be divided into two categories: **1)** pretext task design (Colorization, Jigsaw, PSL) and **2)** contrastive learning (SimCLR, SwAV, BYOL, SimSiam, and Barlow Twins).

Table 4: Comparison with other SSL Methods on SYSU-MM01 (Single-Shot & All-Search).

Method	r1	r10	mAP
Colorization [Zhang <i>et al.</i> , 2016]	30.57	69.02	29.49
Jigsaw [Noroozi and Favaro, 2016]	40.74	82.07	37.71
PSL [Li <i>et al.</i> , 2021]	50.86	86.12	49.35
SimCLR [Chen <i>et al.</i> , 2020]	46.17	84.93	43.38
SwAV [Caron <i>et al.</i> , 2020]	48.25	85.62	45.07
BYOL [Grill <i>et al.</i> , 2020]	52.37	87.34	50.03
SimSiam [Chen and He, 2021]	fail	fail	fail
Barlow Twins [Zbontar <i>et al.</i> , 2021]	51.78	86.45	50.23
MMGL (Ours)	55.05	89.61	53.05

From the results listed in Table 4, we see that Colorization produces modest accuracy on the RGB-IR ReID task. This is because IR images inherently contain no color information. Jigsaw and PSL are more complex but most similar pretext tasks to permutation recovery. Counter-intuitively, they yield suboptimal performance. One possible reason is that the pose variations in person images raise severe spatial misalignment in horizontal direction, rendering them less effective in learning discriminative features than MMGL.

Contrastive learning (CL) methods share similar learning objective with our proposed PCC constraint, namely instance discrimination [He *et al.*, 2020]. They perform better than other pretext tasks, but still attains inferior results than MMGL. Notably, SimSiam even fails to converge on SYSU-MM01. This is because existing CL methods heavily rely on intra-modality data augmentation to create multiple views of the same sample, which does not explicit consider the modality discrepancy in RGB-IR ReID. Instead, PCC utilizes cross-modality cycle-consistency to generate positive patch pairs, leading to more modality-invariant representations.

Moreover, it has been proven that existing CL methods do not work well with small batch sizes [Chen *et al.*, 2020]. However, person ReID is a typical single-GPU task where the efficiency greatly matters. Our proposed paradigm brilliantly exploits body partitions to increase the amount of negative samples with negligible memory costs. Generally, MMGL outperforms state-of-the-art SSL methods consistently.

5 Conclusion

This paper makes the first attempt to investigate the pre-training solution for RGB-IR cross-modality person ReID. To overcome the modality bias issue raised by ImageNet pre-training, we propose a self-supervised MMGL pre-training paradigm that allows ReID models to be pre-trained and fine-tuned directly on existing cross-modality pedestrian datasets, showing superior performance and robustness against over-fitting. By solving a permutation recovery pretext task, MMGL learns highly-invariant representations across modalities. We further propose a part-aware cycle-contrastive learning strategy to learn correspondence between unpaired RGB-IR patches, significantly improving the discriminability of local features. Extensive experiments reveal the effectiveness and transferability of MMGL, even surpassing its ImageNet supervised counterpart without extra data or manual labels.

References

- [Caron *et al.*, 2020] Mathilde Caron, Ishan Misra, Julien Mairal, Priya Goyal, Piotr Bojanowski, and Armand Joulin. Unsupervised learning of visual features by contrasting cluster assignments. *arXiv preprint arXiv:2006.09882*, 2020.
- [Chen and He, 2021] Xinlei Chen and Kaiming He. Exploring simple siamese representation learning. In *Proceedings of the IEEE/CVF Conference on Computer Vision and Pattern Recognition*, pages 15750–15758, 2021.
- [Chen *et al.*, 2020] Ting Chen, Simon Kornblith, Mohammad Norouzi, and Geoffrey Hinton. A simple framework for contrastive learning of visual representations. In *International conference on machine learning*, pages 1597–1607. PMLR, 2020.
- [Chen *et al.*, 2021a] Pengguang Chen, Shu Liu, and Jiaya Jia. Jigsaw clustering for unsupervised visual representation learning. In *Proceedings of the IEEE/CVF Conference on Computer Vision and Pattern Recognition*, pages 11526–11535, 2021.
- [Chen *et al.*, 2021b] Yehansen Chen, Lin Wan, Zhihang Li, Qianyan Jing, and Zongyuan Sun. Neural feature search for rgb-infrared person re-identification. *arXiv preprint arXiv:2104.02366*, 2021.
- [Choi *et al.*, 2020] Seokeon Choi, Sumin Lee, Youngeun Kim, Taekyung Kim, and Changick Kim. Hi-cmd: hierarchical cross-modality disentanglement for visible-infrared person re-identification. In *Proceedings of the IEEE/CVF Conference on Computer Vision and Pattern Recognition*, pages 10257–10266, 2020.
- [Deng *et al.*, 2009] Jia Deng, Wei Dong, Richard Socher, Li-Jia Li, Kai Li, and Li Fei-Fei. Imagenet: A large-scale hierarchical image database. In *2009 IEEE conference on computer vision and pattern recognition*, pages 248–255. Ieee, 2009.
- [Fu *et al.*, 2021] Dengpan Fu, Dongdong Chen, Jianmin Bao, Hao Yang, Lu Yuan, Lei Zhang, Houqiang Li, and Dong Chen. Unsupervised pre-training for person re-identification. In *Proceedings of the IEEE/CVF Conference on Computer Vision and Pattern Recognition*, pages 14750–14759, 2021.
- [Goodfellow *et al.*, 2014] Ian J Goodfellow, Jean Pouget-Abadie, Mehdi Mirza, Bing Xu, David Warde-Farley, Sherjil Ozair, Aaron Courville, and Yoshua Bengio. Generative adversarial networks. *arXiv preprint arXiv:1406.2661*, 2014.
- [Grill *et al.*, 2020] Jean-Bastien Grill, Florian Strub, Florent Altché, Corentin Tallec, Pierre H Richemond, Elena Buchatskaya, Carl Doersch, Bernardo Avila Pires, Zhaohan Daniel Guo, Mohammad Gheshlaghi Azar, et al. Bootstrap your own latent: A new approach to self-supervised learning. *arXiv preprint arXiv:2006.07733*, 2020.
- [He *et al.*, 2019] Kaiming He, Ross Girshick, and Piotr Dollár. Rethinking imagenet pre-training. In *Proceedings of the IEEE/CVF International Conference on Computer Vision*, pages 4918–4927, 2019.
- [He *et al.*, 2020] Kaiming He, Haoqi Fan, Yuxin Wu, Saining Xie, and Ross Girshick. Momentum contrast for unsupervised visual representation learning. In *Proceedings of the IEEE/CVF Conference on Computer Vision and Pattern Recognition*, pages 9729–9738, 2020.
- [Hendrycks *et al.*, 2019] Dan Hendrycks, Norman Mu, Ekin D Cubuk, Barret Zoph, Justin Gilmer, and Balaji Lakshminarayanan. Augmix: A simple data processing method to improve robustness and uncertainty. *arXiv preprint arXiv:1912.02781*, 2019.
- [Hermans *et al.*, 2017] Alexander Hermans, Lucas Beyer, and Bastian Leibe. In defense of the triplet loss for person re-identification. *arXiv preprint arXiv:1703.07737*, 2017.
- [Hjelm *et al.*, 2018] R Devon Hjelm, Alex Fedorov, Samuel Lavoie-Marchildon, Karan Grewal, Phil Bachman, Adam Trischler, and Yoshua Bengio. Learning deep representations by mutual information estimation and maximization. *arXiv preprint arXiv:1808.06670*, 2018.
- [Huang *et al.*, 2021] Yan Huang, Qiang Wu, Jingsong Xu, Yi Zhong, Peng Zhang, and Zhaoxiang Zhang. Alleviating modality bias training for infrared-visible person re-identification. *IEEE Transactions on Multimedia*, 2021.
- [Jang *et al.*, 2016] Eric Jang, Shixiang Gu, and Ben Poole. Categorical reparameterization with gumbel-softmax. *arXiv preprint arXiv:1611.01144*, 2016.
- [Jing and Tian, 2020] Longlong Jing and Yingli Tian. Self-supervised visual feature learning with deep neural networks: A survey. *IEEE Transactions on Pattern Analysis and Machine Intelligence*, 2020.
- [Li *et al.*, 2020] Diangang Li, Xing Wei, Xiaopeng Hong, and Yihong Gong. Infrared-visible cross-modal person re-identification with an x modality. In *Proceedings of the AAAI Conference on Artificial Intelligence*, volume 34, pages 4610–4617, 2020.
- [Li *et al.*, 2021] Zefan Li, Chenxi Liu, Alan Yuille, Bingbing Ni, Wenjun Zhang, and Wen Gao. Progressive stage-wise learning for unsupervised feature representation enhancement. In *Proceedings of the IEEE/CVF Conference on Computer Vision and Pattern Recognition*, pages 9767–9776, 2021.
- [Mena *et al.*, 2018] Gonzalo Mena, David Belanger, Scott Linderman, and Jasper Snoek. Learning latent permutations with gumbel-sinkhorn networks. *arXiv preprint arXiv:1802.08665*, 2018.
- [Nguyen *et al.*, 2017] Dat Tien Nguyen, Hyung Gil Hong, Ki Wan Kim, and Kang Ryoung Park. Person recognition system based on a combination of body images from visible light and thermal cameras. *Sensors*, 17(3):605, 2017.
- [Noroozi and Favaro, 2016] Mehdi Noroozi and Paolo Favaro. Unsupervised learning of visual representations by solving jigsaw puzzles. In *European conference on computer vision*, pages 69–84. Springer, 2016.
- [Sun *et al.*, 2019] Yifan Sun, Liang Zheng, Yali Li, Yi Yang, Qi Tian, and Shengjin Wang. Learning part-based convolutional features for person re-identification. *IEEE transactions on pattern analysis and machine intelligence*, 2019.
- [Wang *et al.*, 2019] Guan'an Wang, Tianzhu Zhang, Jian Cheng, Si Liu, Yang Yang, and Zengguang Hou. Rgb-infrared cross-modality person re-identification via joint pixel and feature alignment. In *Proceedings of the IEEE/CVF International Conference on Computer Vision*, pages 3623–3632, 2019.
- [Wang *et al.*, 2020] Guan-An Wang, Tianzhu Zhang, Yang Yang, Jian Cheng, Jianlong Chang, Xu Liang, and Zeng-Guang Hou. Cross-modality paired-images generation for rgb-infrared person re-identification. In *Proceedings of the AAAI Conference on Artificial Intelligence*, volume 34, pages 12144–12151, 2020.
- [Wu *et al.*, 2017] Ancong Wu, Wei-Shi Zheng, Hong-Xing Yu, Shaogang Gong, and Jianhuang Lai. Rgb-infrared cross-modality person re-identification. In *Proceedings of the IEEE international conference on computer vision*, pages 5380–5389, 2017.
- [Ye *et al.*, 2019] Mang Ye, Xiangyuan Lan, Zheng Wang, and Pong C Yuen. Bi-directional center-constrained top-ranking for visible thermal person re-identification. *IEEE Transactions on Information Forensics and Security*, 15:407–419, 2019.
- [Ye *et al.*, 2020] Mang Ye, Jianbing Shen, David J Crandall, Ling Shao, and Jiebo Luo. Dynamic dual-attentive aggregation learning for visible-infrared person re-identification. *arXiv preprint arXiv:2007.09314*, 2020.
- [Ye *et al.*, 2021a] Mang Ye, Weijian Ruan, Bo Du, and Mike Zheng Shou. Channel augmented joint learning for visible-infrared recognition. In *Proceedings of the IEEE/CVF International Conference on Computer Vision*, pages 13567–13576, 2021.
- [Ye *et al.*, 2021b] Mang Ye, Jianbing Shen, Gaojie Lin, Tao Xiang, Ling Shao, and Steven CH Hoi. Deep learning for person re-identification: A survey and outlook. *IEEE Transactions on Pattern Analysis and Machine Intelligence*, 2021.
- [Zbontar *et al.*, 2021] Jure Zbontar, Li Jing, Ishan Misra, Yann LeCun, and Stéphane Deny. Barlow twins: Self-supervised learning via redundancy reduction. *arXiv preprint arXiv:2103.03230*, 2021.
- [Zhang *et al.*, 2016] Richard Zhang, Phillip Isola, and Alexei A Efros. Colorful image colorization. In *European conference on computer vision*, pages 649–666. Springer, 2016.
- [Zheng *et al.*, 2015] Liang Zheng, Liyue Shen, Lu Tian, Shengjin Wang, Jingdong Wang, and Qi Tian. Scalable person re-identification: A benchmark. In *Proceedings of the IEEE international conference on computer vision*, pages 1116–1124, 2015.
- [Zhong *et al.*, 2020] Zhun Zhong, Liang Zheng, Guoliang Kang, Shaozi Li, and Yi Yang. Random erasing data augmentation. In *Proceedings of the AAAI Conference on Artificial Intelligence*, volume 34, pages 13001–13008, 2020.
- [Zhu *et al.*, 2017] Jun-Yan Zhu, Taesung Park, Phillip Isola, and Alexei A Efros. Unpaired image-to-image translation using cycle-consistent adversarial networks. In *Proceedings of the IEEE international conference on computer vision*, pages 2223–2232, 2017.
- [Zou *et al.*, 2018] Yuliang Zou, Zelun Luo, and Jia-Bin Huang. Df-net: Unsupervised joint learning of depth and flow using cross-task consistency. In *Proceedings of the European conference on computer vision (ECCV)*, pages 36–53, 2018.